J. Phycol. **48,** 1494–1509 (2012)

DOI: 10.1111/jpy.12004

PRODUCTION AND CHARACTERIZATION OF THE INTRA- AND EXTRACELLULAR CARBOHYDRATES AND POLYMERIC SUBSTANCES (EPS) OF THREE SEA-ICE DIATOM SPECIES, AND EVIDENCE FOR A CRYOPROTECTIVE ROLE FOR EPS[1]

Shazia N. Aslam, Tania Cresswell-Maynard

School of Biological Sciences, University of Essex, Wivenhoe Park, Colchester CO4 3SQ, UK

David N. Thomas

Ocean Sciences, College of Natural Science, Bangor University, Menai Bridge, Anglesey LL59 5AB, UK
Finnish Environment Institute (SYKE), Marine Research Centre, P.O. Box 140, Helsinki FI-00251, Finland

and Graham J. C. Underwood[2]

School of Biological Sciences, University of Essex, Wivenhoe Park, Colchester CO4 3SQ, UK

Diatoms and their associated extracellular polymeric substances (EPS) are major constituents of the microalgal assemblages present within sea ice. Yields and chemical composition of soluble and cell-associated polysaccharides produced by three sea-ice diatoms, *Synedropsis* sp., *Fragilariopsis curta*, and *F. cylindrus*, were compared. Colloidal carbohydrates (CC) contained heteropolysaccharides rich in mannose, xylose, galactose, and glucose. *Synedropsis* sp. CC consisted mainly of carbohydrates <8 kDa size, with relatively soluble EPS, compared to high proportions of less-soluble EPS produced by both *Fragilariopsis* spp. *F. curta* colloidal EPS contained high concentrations of amino sugars (AS). Both *Fragilariopsis* species had high yields of hot bicarbonate (HB) soluble EPS, rich in xylose, mannose, galactose, and fucose (and AS in *F. cylindrus*). All species had frustule-associated EPS rich in glucose–mannose. Nutrient limitation resulted in declines in EPS yields and in glucose content of all EPS fractions. Significant similarities between EPS fractions from cultures and different components of natural EPS from Antarctic sea ice were found. Increased salinity (52) reduced growth, but increased yields of EPS in *Fragilariopsis cylindrus*. Ice formation was inhibited by *F. cylindrus*, EPS, and by enhanced EPS content (additional xanthan gum) down to −12°C, with growth rate reduced in the presence of xanthan. Differences in the production and composition of EPS between *Synedropsis* sp. and *Fragilariopsis* spp., and the association between EPS, freezing and cell survival, supports the hypothesis that EPS production is a strategy to assist polar ice diatoms to survive the cold and saline conditions present in sea ice.

Key index words: **cryoprotection; dissolved carbohydrates; exopolymers; extracellular polymeric substances; polar diatoms; sea ice**

Sea ice occupies up to 13% of the earth's surface, and plays a significant role in the ecology and biogeochemistry of the polar and several subpolar regions (Thomas and Dieckmann 2002). A diverse group of microalgae grow to high standing stocks within, and on the peripheral surfaces of, sea ice (Arrigo et al. 2010). Algal growth can be rapid during sea-ice formation in autumn, especially at the porous ice–seawater interface, and then slows, with cell metabolism altering in response to changing conditions within the developing ice matrix (nutrient limitation, increasing salinity, and lowering irradiance) during the onset of winter (Gleitz and Thomas 1992, 1993, Krell et al. 2008). Algal growth resumes when light levels increase in the polar spring (Søgaard et al. 2010, Petrou and Ralph 2011).

Substantial concentrations of particulate and dissolved extracellular polymeric substances (EPS) have been measured in most types of sea ice (Underwood et al. 2010, Juhl et al. 2011, Krembs et al. 2011, Aslam et al. 2012). These polysaccharide-rich mucilages form an organic network within the ice, modifying the structure of brine channels and influencing the development of the sea-ice matrix (Krembs et al. 2002, 2011, Juhl et al. 2011). The chemical composition of sea-ice EPS is largely uncharacterized, although particulate EPS are predominantly acidic polysaccharides (McConville et al. 1985, 1999, Meiners et al. 2003, Mancuso Nichols et al. 2005), whereas dissolved EPS comprise a range of different heteropolymers with varying monosaccharide, uronic acid, and solubility characteristics (McConville et al. 1985, 1999, Underwood et al. 2010, Aslam et al. 2012). As physicochemical properties play a major role in determining the solubility and binding potential of EPS (Suzuki and Tanaka 1990, Chen and Hoffman 1995, Krembs and Deming 2008, Verdugo 2012), characterizing the EPS produced by sea-ice microflora is a necessary step to

[1]Received 29 November 2011. Accepted 9 May 2012.
[2]Author for correspondence: e-mail gjcu@essex.ac.uk.

understanding the role of EPS in the biogeochemistry and ecology of sea ice.

Diatoms produce a diverse range of polysaccharide-rich EPS containing uronic acids, sulfated sugars, and protein (Hoagland et al. 1993, Chiovitti et al. 2003, 2005, Underwood and Paterson 2003, Abdullahi et al. 2006). Pennate diatoms and other microorganisms alter the production rates and chemical characteristics of their EPS in response to inorganic nutrient limitation, salinity, and low temperature stress (Smith and Underwood 2000, Underwood et al. 2004, Abdullahi et al. 2006, Apoya-Horton et al. 2006, Nevot et al. 2008, Marx et al. 2009, Mishra and Jha 2009). Such physiological flexibility may enable pennate diatoms to modify their surrounding microenvironment by altering the properties of their EPS as cells are exposed to changing conditions as sea ice consolidates (Thomas et al. 2010). The only detailed study of EPS production for a polar diatom found that *Stauroneis amphyioxys* produced charged and sulfated heteropolysaccharides, which changed in composition between logarithmic growth and stationary phase conditions (McConville et al. 1999).

This study quantified and characterized both soluble and cell-associated polysaccharides produced by three diatom species with global polar distributions: *Synedropsis* sp. (ccmp2745) (Grunow) Hasle, Medlin & Syvertsen, *Fragilariopsis curta* (van Heurck), Hustedt, and *Fragilariopsis cylindrus* (Grunow), Kreiger (Round et al. 1990, Stickley et al. 2009). *F. cylindrus* and *F. curta* are often dominant species within pack sea ice and platelet layers (Gleitz et al. 1998, Günther and Dieckmann 2001, Thomas et al. 2001) with *F. cylindrus* thriving equally well in the water column and sea ice (Kang and Fryxell 1992), whereas *Synedropsis* species are mostly found only at the ice–seawater interface on the lower surfaces of ice floes (Hasle et al. 1994). We hypothesized that if EPS are involved in protecting cells from conditions of low temperature and high salinity, then *Fragilariopsis* spp. (that live within the sea-ice matrix) should produce EPS that are larger, more insoluble, and biochemically more complex than EPS produced by *Synedropsis* spp. We investigated the effect of salinity on carbohydrate production and the potential of extracellular polysaccharides to protect cells from freezing, exposing cultures of *F. cylindrus* grown at salinity 34 and 52, to incremental 4°C temperature reductions from 0°C down to −20°C over a 55 d period, and also in the presence of additional EPS (the heteropolysaccharide xanthan gum). If EPS helps in cell survival in brines at low temperatures and high salinities, *Fragilariopsis* in culture should produce more EPS under such conditions, and that the presence of high concentrations of additional EPS should alter the freezing characteristics of the media (Krembs et al. 2011) permitting continued algal growth.

MATERIALS AND METHODS

Culture conditions. *Synedropsis* sp. (ccmp2745), *F. curta* (provided by G. S. Dieckmann, Alfred-Wegener-Institute, Bremerhaven, Germany), and *F. cylindrus* (provided by T. Mock, UEA, Norwich, UK) were used for this study. *Synedropsis* sp. cultures were maintained in LI medium (nitrate concentration 0.9 mmol $\cdot$ L^{-1}) with additional silicate (Guillard and Hargraves 1993), and *Fragilariopsis* spp. were grown in enriched artificial seawater (EASW, Berges et al. 2001) with 1.1 mmol $\cdot$ L^{-1} final nitrate concentrations. All cultures were grown at a salinity of 34, at 0°C, under continuous illumination (71 μmol photons $\cdot$ m^{-2} $\cdot$ s^{-1}). To obtain axenic cultures, cell inocula were incubated in media containing penicillin/streptomycin solution (100,000 units penicillin and 100 mg $\cdot$ L^{-1} streptomycin, Sigma) and gentamycin (33 mg $\cdot$ L^{-1}) for 48 h, after which fresh sterile media was added to each flask, and cells grown on at 0°C to provide cells for experimentation. Regular examination of cultures by light microscopy revealed no visible bacteria contamination.

EXPERIMENT 1: EFFECT OF GROWTH PHASE ON PHOTOPHYSIOLOGY, CARBOHYDRATE, AND EPS PRODUCTION AND COMPOSITION

Cultures of each species were grown axenically in triplicate 5 L flasks, each containing 2 L of media and a starting inoculum of 2×10^9 cells in 20 mL, taken from actively growing axenic stock cultures. Cells were prevented from sticking to the flask sides by gently rotating flasks once a day. Cultures were grown for 24 d (*Synedropsis* sp.) and 28 d (*Fragilariopsis* spp.), and sampled at the same time of day on seven occasions (Fig. 1). During sampling cultures were resuspended, and subsamples were taken for measurements of cell density using a haemocytometer, cell photophysiology, carbohydrate content, and biochemical composition (see below). Intrinsic growth rate (μ) was calculated from the logistic growth equation (Levasseur et al. 1993).

Changes in the characteristics of PSII photochemistry in the three diatom species were determined at each sampling occasion throughout Experiment 1. Cultures were dark adapted for 30 min at 0°C, before 3 mL subsamples of suspended cultures were taken and measured immediately using a Satlantic FIRe fluorometer (Satlantic Inc., Halifax, NS, Canada) at room temperature. Excitation was produced from a high luminosity blue and green (450 and 500 nm peak heights, respectively) light-emitting diode array. Each acquisition consisted of a four step transient determining single turnover (ST) excitation from a 100 μs pulse, ST relaxation over 500 ms, multiple turnover (MT) excitation from a 600 ms pulse, and MT relaxation over 1 s. Twenty sequential measurements were averaged to increase the signal to noise ratio (Suggett et al. 2008). Using FIREPRO software (Satlantic Inc.), the maximum PSII photochemical efficiency (F_v/F_m), the functional absorbance cross-section of PSII (σ_{PSII}), and the rate of reoxidation of the primary quinine acceptor (τ_{QA}) were calculated (Kromkamp and Forster 2003, Suggett et al. 2008).

EXPERIMENT 2: EFFECT OF SALINITY AND THE PRESENCE OF EXTRACELLULAR POLYMERS (XANTHAN GUM) ON FRAGILARIOPSIS CYLINDRUS GROWTH UNDER INCREMENTAL COLD STRESS

Fragilariopsis cylindrus cultures were acclimated and grown at two salinities (EASW adjusted with NaCl to give salinities of 34 and 52) for a 2-month

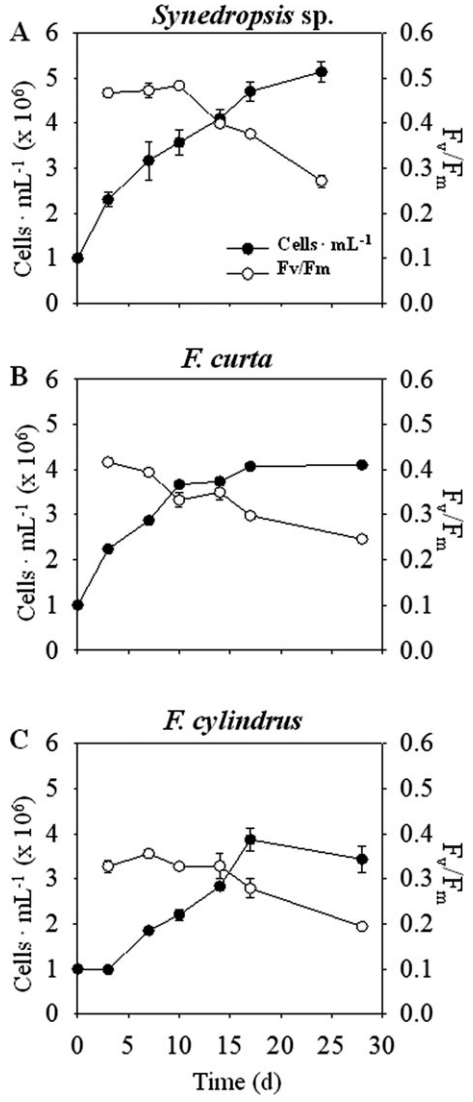

FIG. 1. Cell density and maximum PSII photochemical efficiency (F_v/F_m) of (A) *Synedropsis* sp., (B) *Fragilariopsis curta*, and (C) *F. cylindrus* in cultures grown over 24 and 28 d *Synedropsis* and *Fragilariopsis* species, respectively (mean ± standard error, $n = 3$ for each time point).

period prior to the experiment. Three treatments (0 addition–control) and +1 and +5 g · L^{-1} of the high molecular weight polysaccharide (xanthan gum; Sigma-Aldrich Co., St. Louis, MO, USA) were established in triplicate 250 mL flasks, containing 150 mL media each for each salinity condition, with all flasks subjected to incremental −4°C decreases in temperature from 0 to −20°C over a 56 d period. To reduce the potential for nutrient limitation, a semibatch culture approach was used: on d 10 (salinity 34 treatments) and d 23 (salinity 52 treatments), all flasks were diluted (1:1) with fresh media. Flasks were rotated to bring all cells into suspension, and half of the volume was withdrawn and replaced by the same volume of fresh media containing the same xanthan concentration.

Experiments started at 0°C under continuous illumination (71 μmol photons · m^{-2} · s^{-1}), with the first temperature reduction to −4°C being made 13 d after inoculation. Temperatures were further decreased to −8°C on d 26, to −12°C on d 39, and to −20°C on d 52. The experiment was terminated on d 56 when all flasks had become frozen. The variation in temperature conditions throughout the experiment was ±1°C. Subsamples for cell enumeration were taken from each flask on d 13, 26, 39, and 52 (before the decrease in temperature). No cell counts were made on d 55 as cultures were completely frozen at this stage. On d 56 the cultures were defrosted and centrifuged; both cells and supernatants were used for carbohydrate analysis as described below.

Extraction of carbohydrate fractions. Using established sequential extractions (Wustman et al. 1997, Smith and Underwood 2000, Chiovitti et al. 2003, Abdullahi et al. 2006) diatom EPS were fractionated into:

1. A soluble (colloidal) fraction containing both polymeric (colloidal EPS) and nonpolymeric (lower molecular weight) carbohydrates secreted by cells into the culture media and that were no longer cell associated.
2. A hot water (HW)-extracted carbohydrate fraction containing predominantly intracellular storage polysaccharides (mainly glucans), though there is some extraction of external EPS coating the cells.
3. A hot bicarbonate (HB)-extracted fraction that solubilizes the relatively gelatinous and water-insoluble extracellular polysaccharides, removing most of the mucilage from the surface of the diatom frustule.
4. A hot alkali extraction that dissolves the silica cell wall and liberates EPS intimately linked with the silica frustule.

Each extraction required approximately 80–200 mL of culture. These volumes were removed from the main flasks on d 0, 3, 10, 14, 17, 24 for *Synedropsis* and d 28 for the *Fragilariopsis* species and taken through the following stepwise procedures:

Colloidal carbohydrate (*CC*) *fraction:* Samples were centrifuged at 4000*g* for 15 min and the supernatant (the CC fraction) was removed.

HW fraction: Cell pellets from the CC extractions were resuspended in 34 g · L^{-1} NaCl (at a concentration of 10^7–10^8 cell · mL^{-1}), and were incubated at 100°C for 1 h. After cooling to room temperature samples were centrifuged (3500*g*, 15 min). The supernatant (HW fraction) was carefully removed.

HB fraction: Cell pellets remaining from the HW extraction procedure were extracted with 0.5 M $NaHCO_3$ by incubating at 100°C for 1 h.

Hot alkali (*HA*) *fraction*: The most insoluble polymers were extracted with 1 M NaOH and 0.2 M $NaBH_4$ at 100°C for 1 h.

An aliquot (1 mL) of each extracted fraction (CC, HW, HB, and HA) was used to determine

carbohydrate concentration (phenol sulfuric acid assay). The remaining material was dialyzed overnight (at 20°C) through 8 kDa dialysis tubing against ultra pure water (18.2 MΩ cm, MilliQ) under moderate stirring, to reach a final salinity <1. Desalted samples were freeze dried for EPS partitioning (the colloidal fraction) and determination of monosaccharide composition (CC, HW, HB, and HA).

Dissolved EPS (dEPS) fractionation. Dialyzed and freeze-dried CC fractions were redissolved in ultra pure water (giving a concentration factor of 20 relative to the original volume). This fraction was termed colloidal polysaccharides (CPs). Redissolved CPs samples were divided into four aliquots of 1–4 mL each. One aliquot was used to determine carbohydrate and amino-sugar concentrations, and monosaccharide content (described later). The remaining three aliquots were used to isolate EPS components with different solubility by precipitation with 30%, 50%, and 70% ethanol overnight at 4°C. The precipitates from each ethanol treatment were recovered by centrifugation (3500*g*, 15 min), air dried and redissolved in ultra pure water (0.65 mL). These precipitated EPS fractions were named as EPS-30, EPS-50, and EPS-70 (based on the ethanol percentage used for precipitation, Underwood et al. 2010, Aslam et al. 2012). The terms % $CHO_{0–30}$ (highly insoluble EPS), % $CHO_{50–30}$ (soluble EPS), % $CHO_{70–50}$ (highly soluble EPS), and % $CHO_{100–70}$ (non-EPS) refer to the percentage contribution of dEPS and non-EPS carbohydrate fractions relative to the total dissolved carbohydrate (dCHO) concentration, and were calculated as described by Underwood et al. (2010).

Carbohydrate (CHO) analysis. Carbohydrate concentrations were determined using a modified phenol sulfuric acid assay (Dubois et al. 1956) as described by Underwood et al. (2010). Carbohydrate concentrations obtained by this assay were termed phenol sulfuric acid assay analyzed-carbohydrates (PSA-CHO). Glucose was used as a standard with concentrations reported as mg glucose equivalents. PSA-CHO were determined before (CC) and after dialysis (CPs).

Concentrations of AS were determined (Ferrieres et al. 2007) in the dialyzed carbohydrate extracts (CPs). Samples were hydrolyzed overnight at 100°C in 0.5 N HCl. After hydrolysis, samples were freeze dried to remove acid and were dissolved in ultra pure water for analysis. *N*-acetylglucosamine was used as standard.

The detection limits were 5 $\mu g \cdot mL^{-1}$ glucose and 20 $\mu g \cdot mL^{-1}$ *N*-acetylglucosamine for the phenol sulfuric acid assay and AS, respectively. The coefficient of variation (CV, standard deviation/mean) in all assays was <1%.

The phenol sulfuric acid assay is a general method used for carbohydrate quantification, but it does not detect AS, so the carbohydrate yields for each fraction (CHO_{CC}, CHO_{HW}, CHO_{HB}, and CHO_{HA}; carbohydrate concentrations of CC, HW, HB, and HA fractions, respectively) were calculated by adding together PSA-CHO and AS (PSA-CHO + AS). Overall carbohydrate yields (sum of all fractions, ΣCHO) produced by each diatom species were calculated by adding carbohydrate yields for each fraction, that is, $CHO_{CC} + CHO_{HW} + CHO_{HB} + CHO_{HA}$ separately for both active and stationary growth phases.

To relate xanthan gum concentrations to measures of carbohydrates, interconversion of xanthan ($\mu g \cdot mL^{-1}$) to glucose ($\mu g \cdot mL^{-1}$) was conducted as described by van der Merwe et al. (2009). Standards of known concentrations (0–100 $\mu g \cdot mL^{-1}$) of xanthan and glucose were prepared, analyzed by phenol sulfuric acid assay, and a model II regression was used to determine the calibration relationship ($r^2 = 0.993$). The intercalibration allowed the conversion of xanthan ($\mu g \cdot mL^{-1}$) to glucose ($\mu g \cdot mL^{-1}$) using the following equation:

$$\text{xanthan}(\mu g \cdot mL^{-1}) = 0.676 \times (\text{glucose}\, \mu g \cdot mL^{-1}) + 0.0013$$

Monosaccharide composition of carbohydrate fractions. Neutral monosaccharide composition was determined by gas chromatography linked with mass spectroscopy (GC-MS). Polysaccharides and standards were hydrolyzed with 200 μL of 2 $mol \cdot L^{-1}$ trifluoroacetic acid at 100°C for 3 h, dried under a clean stream of nitrogen at 40°C, saponified with 1 $mol \cdot L^{-1}$ ammonia (50 μL), and then reduced to the corresponding alditols using 500 μL sodium borohydrate-dimethyl sulfoxide. The reaction was quenched with 50 μL of glacial acetic acid for 10 min at room temperature. Alditols were acetylated with 1-methylimidazole (100 μL) and acetic anhydride (1 mL) for 15 min at room temperature, the reaction quenched with 500 μL water, and extracted with 500 μL of HPLC grade dichloromethane. These derivatized monosaccharide mixtures were dried under clean nitrogen gas at 40°C and redissolved in 50–250 μL of HPLC grade dichloromethane (depending upon concentration). Three microliter of each sample was injected into a Finnigan Trace GC Ultra DSQ quadrupole GC-MS. Monosaccharide separation was carried out using a RT-2330 column with a temperature gradient of 65°C for 0 min, increasing by $8°C \cdot min^{-1}$ to 240°C for 2 min, then increasing by $4°C \cdot min^{-1}$ to 250°C for 10 min. Inositol was used as the internal standard. Response factors were calculated for each sugar with respect to inositol, and monosaccharides were identified according to their retention time, response factor, and mass spectra, and were quantified using rhamnose (Rha), fuctose (Fuc), ribose (Rib), arabinose (Arab), xylose (Xyl), mannose (Man), galactose (Gal), glucose (Glc), and inositol as standards that underwent the same hydrolyzation and acetylation procedure. The CV among replicate subsam-

ples for the derivitization and measurement by GC-MS was <5%.

Data and statistical analysis. To compare differences in carbohydrate and EPS production and composition between species, and between cells in different physiological states, we grouped data for each species into two periods, that is, active growth phase and stationary phase, on the basis of changes in cell density, and patterns in photophysiology (F_v/F_m, σ_{PSII}, τ_{QA}), giving periods of active growth (d 3, 7, 10, 14, and 17 for *Synedropsis,* d 3, 7, 10, and 14 for *F. curta,* and d 7, 10, and 14 for *F. cylindrus*) and stationary phase (d 24 for *Synedropsis*, d 17 and 28 for *F. curta,* and d 17 and 28 for *F. cylindrus*) for each species.

Statistical analyses were conducted using SPSS® 18.0 (IBM Corporation, NY, USA). Significant differences were determined using *t*-test and analysis of variance (ANOVA, with Tukey's post hoc tests). Normality of the samples was checked, but the assumption of normality could not be rejected in any case. All statistically significant differences quoted are at $P \leq 0.05$. Standard error (SE) is presented as a measure of variability for all samples. PERMANOVA Permutational Multivariate Analysis of Variance analysis for EPS profiles were carried out in Primer 6, whereas principal component and cluster analysis of the relative monosaccharide composition were carried out using MVSP v3.1 (Kovach Computing Services, Anglesey, Wales).

RESULTS

Culture growth rates and changes in photophysiology. Cell density (Fig. 1A–C) significantly increased over the growth period for all three species ($F_{6,14} = 33.7$ or greater, all at $P \leq 0.05$). Maximum cell densities (at $P < 0.01$) were reached by *Synedropsis* (5.13×10^6 cells $\cdot$ mL^{-1}), with a maximum growth rate ($\mu \pm$ SE) of 0.28 d^{-1} ± 0.02 during d 0 to 3, and a minimum growth rate of 0.01 d^{-1} ± 0.002 between d 17 and 24 (Fig. 1A). *Synedropsis* showed no decline in F_v/F_m until after d 10, after which F_v/F_m significantly declined (in a linear fashion at approximately 2% d^{-1}) until the end of the experiment at d 24 (Fig. 1A). F_v/F_m was negatively correlated with σ_{PSII} over the 24 d period ($r_{18} = -0.56$, $P < 0.05$), and turnover time of QA (τ_{QA}) showed a significant increase from ≈1500 to ≈2000 μS between d 7 and 10 (Fig. S1, see Supporting Information). Reductions in growth rates and the significant drop in F_v/F_m (to 50% of its starting value) by d 24 indicated the onset of stationary phase.

Both *Fragilariopsis* species showed similar growth curve patterns, reaching maximum cell densities (4×10^6 and 3.4×10^6 cells $\cdot$ mL^{-1} for *F. curta* and *F. cylindrus*, respectively) after 17 d of growth (Fig. 1B and C). *F. curta* showed the highest rates of growth during the first 10 d ($\mu = 0.27$ d^{-1} ± 0.01 from d 0 to d 3), after which growth rates declined to a minimum rate (0.001 d^{-1} ± 0.001, stationary phase) between d 17 and 28 (Fig. 1B). F_v/F_m gradually declined in *F. curta* cultures, correlated with a significant rise (by d 10) in σ_{PSII} values over the 28 d period ($r_{18} = -0.72$, $P < 0.001$, Fig. S1). The reductions in growth rate, F_v/F_m, and increases in σ_{PSII} indicate that *F. curta* was experiencing nutrient limitation and was in stationary phase after 14 d of growth. After a 3 d lag phase, *F. cylindrus* growth rate reached a maximum of 0.16 d^{-1} ± 0.01 between d 3 and 7 (Fig. 1C). There were no further increases in cell density after d 17, a change coinciding with significant declines in F_v/F_m, and a rise in σ_{PSII} (correlation between F_v/F_m and σ_{PSII}, $r_{15} = -0.68$, $P < 0.01$; Fig. S1), indicating nutrient limitation and cessation of growth.

Carbohydrate yields and monosaccharide profiles of soluble and cell-associated carbohydrate fractions. Colloidal extracellular carbohydrates: All three diatoms species produced substantial amounts of extracellular CC, with significantly higher yields (pg C $\cdot$ cell^{-1}) of CHO_{CC} than in the HW, HB, or HA fractions ($F_{3,17} = 17.0$, $F_{3,16} = 48.1$, and $F_{3,15} = 10.4$, $P \leq 0.001$ in all cases, for *Synedropsis* sp., *F. curta,* and *F. cylindrus,* respectively). CC (PSA sugars and AS combined) contributed over 50% to the sum of carbohydrate (ΣCHO) produced by each species (Table 1). A consistent pattern for all species was a significant decline in yield per cell of CC (both PSA-CHO and AS components) when cells entered stationary phase (Fig. 2A and B; Table 1).

Synedropsis sp. produced significantly higher concentrations of colloidal PSA-CHO per cell compared to both *Fragilariopsis* species, ($F_{2,23} = 4.1$ and $F_{2,8} = 10.3$, *t* $P \leq 0.05$, for growth and stationary phases, respectively). The CC of *Synedropsis* had low amino-sugar content, ~8% of the total carbohydrate (Fig. 2B). A similar balance was present (8% amino sugar) in the CC produced by *F. cylindrus*. In contrast, *F. curta* produced significantly higher yields of AS compared to the other two species ($F_{2,11} = 22.8$ and $F_{2,8} = 26.7$ in growth and stationary phases, respectively, at $P < 0.001$) during active growth, and when in stationary phase, with approximately equal proportions of PSA-CHO and AS in its CC (Fig. 2A and B; Table 1).

The proportion of polysaccharides (CPs, after dialysis, Fig. 3A) in the colloidal fraction was highest in *F. cylindrus* (>67%, Table 1). In comparison, only 20% of the high yield of CC produced during active growth by *Synedropsis* sp. consisted of polysaccharides ≥8 kDa (Fig 3A). During active growth, *F. curta* produced extracellular CC consisting of 35% polysaccharides, and 65% small molecular weight carbohydrates <8 kDa. Despite these differences between species in the amount and proportion of polysaccharides produced during active growth, all three taxa showed increases in concentrations of polysaccharides ≥8 kDa when in stationary phase, with the proportion of polysaccharide

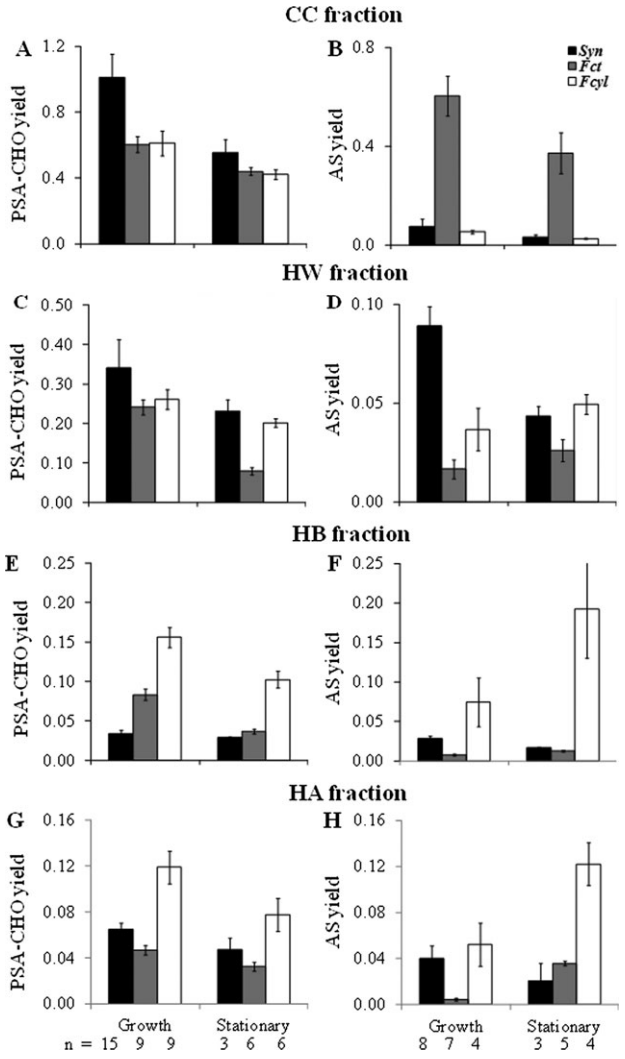

FIG. 2. Average yield (pg C · cell^{-1}) of phenol sulfuric acid quantified carbohydrates (PSA-CHO) and amino sugars (AS) in (A, B) dialyzed colloidal (CC), (C, D) hot water (HW), (E, F) hot bicarbonate (HB), and (G, H) hot alkali (HA) extracts from *Synedropsis* (*Syn*), *Fragilariopsis curta* (*Fct*), and *F. cylindrus* (*Fcyl*) during periods of either active growth or stationary phase (mean ± standard error).

increasing to 61, 39, and 78% for *Synedropsis* sp., *F. curta*, and *F. cylindrus*, respectively (Fig. 3A).

Ethanol solubility-based EPS fractionation showed significant differences between the diatom species in the proportions of highly insoluble, less-soluble, and non-EPS polysaccharides in their CPs (Fig. 3B). The CPs of *Synedropsis* sp. consisted of up to 74% non-EPS or highly soluble EPS (% $CHO_{70–100}$ and % $CHO_{50–70}$ components), significantly higher proportions that for the comparable polysaccharides of *F. curta* or *F. cylindrus*. In contrast, the CPs produced by both *Fragilariopsis* species consisted of significantly higher proportions of the most insoluble, highly complex EPS (% $CHO_{0–30}$; Fig. 3B), and the majority (65% and greater) of their polysaccharides consisting of EPS of varying solubility rather than non-EPS polysaccharides.

When *Synedropsis* sp. entered stationary phase, the proportion of % $CHO_{30–50}$ significantly decreased (7-fold) with an increase in less complex (% $CHO_{50–70}$) and non-EPS polysaccharides (% $CHO_{70–100}$). Conversely, *F. curta* showed an increase in the percentage contribution of highly insoluble EPS (% $CHO_{0–30}$) in its CPs when in stationary phase (Fig. 3B). Overall, *F. cylindrus* had the highest contribution (up to 80%) of EPS (% $CHO_{0–30}$ + % $CHO_{30–50}$ + % $CHO_{50–70}$) in its CP fraction, followed by *F. curta* (up to 70%) and then *Synedropsis* sp. (up to 63%). PERMANOVA revealed significant differences between *Synedropsis* and the two *Fragilariopsis* species in the percentage contribution of the different colloidal EPS fractions ($F_{2,29} = 23.11$ at $P < 0.001$); the proportions of % $CHO_{0–30}$ (highly insoluble EPS) followed by the % $CHO_{50–70}$ (most soluble EPS) fraction being responsible for most of the dissimilarity between *Synedropsis* and *Fragilariopsis* species (SIMPER analysis).

Generally, all three species produced extracellular colloidal heteropolysaccharides with Glc, Man, Gal, and Xyl as major contributing sugars (Fig. 4A). The ratios of monosaccharides in the CC-CPs fraction differed for each species, e.g., the relative contribution of Glc was up to 57% in the *Synedropsis* sp. CC fraction but only 30% and 25% for *F. curta* and *F. cylindrus*, respectively. The monosaccharide composition of the CC fraction also changed with cell growth phase. In *Synedropsis*, the relative abundance of Man (17%–6%) and Xyl (8.3%–4.1%) decreased (t-test$_{(6)} = 2.9$ and 2.7 at $P < 0.05$ for Xyl and Man, respectively) with corresponding increases in Glc and Gal from the growth to stationary phase. Similarly, the relative abundance of Glc declined from growth to stationary phase in the CC fractions produced by both *Fragilariopsis* species, associated with a 2-fold increase in Man for *F. curta* and Xyl in *F. cylindrus* (Fig. 4A; Table 1).

Cell-associated intra- and extracellular carbohydrates: *Synedropsis* sp. produced significantly higher concentrations of HW extractable carbohydrate (CHO_{HW}) per cell, when compared to both of the *Fragilariopsis* species ($F_{2,23} = 4.01$ at $P < 0.05$) during active growth (Fig. 2C). There were significant declines ($P < 0.05$) in HW PSA-CHO yields (pg C · cell^{-1}) in stationary phases for all species, with the lowest yields ($F_{2,8} = 4.01$ at $P < 0.01$) produced by *F. curta* in comparison to *Synedropsis* and *F. cylindrus* (Fig. 2C). Associated with these changes were decreases in the relative abundance of Glc in the stationary phase HW (64%–58%, 52%–40%, and 60%–53% of total monosaccharides from growth phase to stationary phase in *Synedropsis*, *F. curta*, and *F. cylindrus*, respectively; Fig. 4B). Amino-sugar content was up to 11-fold less than PSA-CHO_{HW} for all species (Table 1). For cells in stationary phase, AS decreased 3-fold in *Synedropsis*

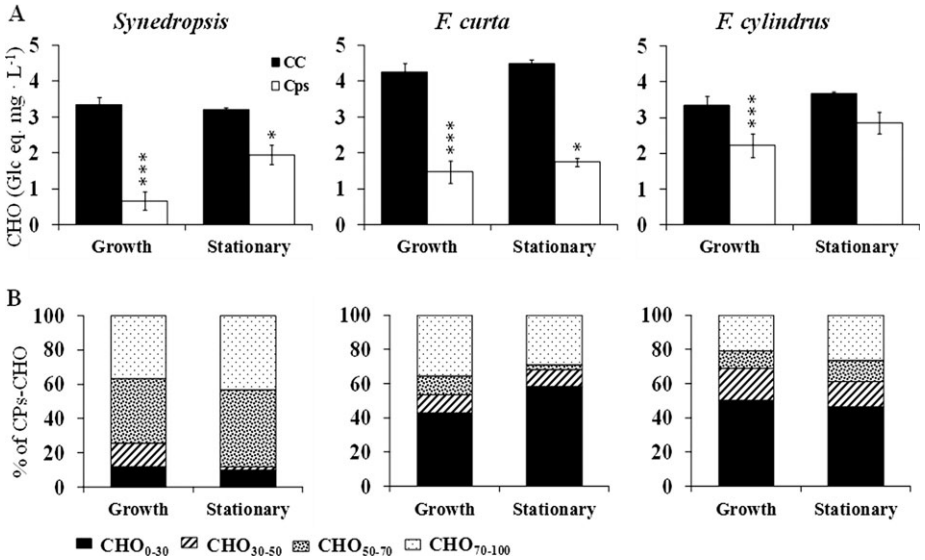

FIG. 3. (A) Concentrations of phenol sulfuric acid quantified carbohydrates (PSA-CHO, eq. to mg · L^{-1} Glc) in colloidal carbohydrate (CC) and colloidal polysaccharides (CPs) fractions produced by *Synedropsis* (*Syn*), *Fragilariopsis curta* (*Fct*), and *F. cylindrus* (*Fcyl*) and (B) solubility-based (ethanol-precipitated) EPS profiles from CPS produced by all diatom species during periods of either active growth or stationary phase (mean ± standard error, $n = 15$, three for *Synedropsis* sp; nine and six for *Fragilariopsis* spp. for growth and stationary phase periods, respectively). Significant decreases in carbohydrate concentration after dialysis at $^{*}P < 0.05$, and $^{***}P < 0.001$, are indicated.

cultures ($t\text{-test}_{(8)} = 2.367$, $P < 0.05$), whereas AS concentrations increased ($t\text{-test}_{(5)} = 2.8$ at $P < 0.05$) by a similar proportion in *F. cylindrus* cultures (Fig. 2D).

Hot water fractions in all species were enriched with glucose, with Glc generally exceeding 50% of total monosaccharides (Fig. 4B). In contrast to the composition of the other carbohydrate fractions, the relative abundance of Rib was significantly ($P < 0.001$) higher in the HW fraction extracted from all three diatom species, particularly in the HW fraction extracted from *Fragilariopsis* species where Rib was the second most abundant monosaccharide after Glc (18% and 15% in *F. curta* and *F. cylindrus*, respectively; Fig. 4B).

Yields of cell-bound extracellular EPS isolated using HB digestion were substantially lower than CC or HW yields for all three species (Fig. 2E). *F. cylindrus* produced significantly higher yields in comparison to *Synedropsis* sp. and *F. curta*, ($F_{2,42} = 49.1$ and $F_{2,25} = 11.2$ for PSA-CHO and AS, respectively, $P < 0.001$). Yields of PSA-CHO in HB fractions decreased in stationary phase in all species ($P < 0.01$), but there were significant increases ($P < 0.05$) in AS in both *Fragilariopsis* species in stationary phase (by 2- and 4-fold for *F. curta* and *F. cylindrus,* respectively, Fig. 2F). This increase resulted in the HB carbohydrate present surrounding *F. cylindrus* cells in stationary phase consisting of over 62% of AS (Table 1).

The monosaccharide composition of HB extracted from *Fragilariopsis* species in active growth was significantly different ($P < 0.05$) from that of *Synedropsis* due to differences in Man, Gal, and Rha. The highest abundance of Gal was present in *Synedropsis* HB fractions ($F_{6,62} = 110.7$, $P < 0.001$), whereas both *Fragilariopsis* species had Man as the most abundant monosaccharide in their HB carbohydrate ($F_{6,28} = 42.25$ and 20.00 at $P < 0.001$, *F. curta* and *F. cylindrus,* respectively; Fig. 4C). Both *Synedropsis* sp. and *F. curta* showed reductions in the relative abundance of Man between active growth and stationary phases. In *Synedropsis* HB, Man decreased ($t_{(7)} = 2.9$ at $P < 0.05$) and Fuc increased in relative abundance ($t_{(7)} = 2.5$ at $P < 0.05$). In *F. curta* HB, the relative abundance of Man decreased ($t_{(4)} = 3.4$ at $P < 0.05$) with increase in Rha ($t_{(4)} = 5.6$ at $P < 0.01$) and Fuc ($t_{(4)} = 8.1$ at $P < 0.001$, Fig. 4C; Table 1).

The yields of frustule-associated carbohydrate extracted with HA were significantly higher in *F. cylindrus* compared to *Synedropsis* and *F. curta* (PSA-CHO, $F_{2,43} = 17.96$, $P < 0.0001$; AS, $F_{2,20} = 13.2$, $P < 0.0001$; Fig. 2G). *Synedropsis* produced a HA fraction dominated by Xyl, Gal, Man, and Glc, which was stable in terms of yield (both PSA-CHO and AS) and monosaccharide content (Fig. 4D) between growth and stationary phases. The HA fractions of *F. curta* and *F. cylindrus* were dominated by Man and Glc (Fig. 4D). Both *Fragilariopsis* species showed a decline in PSA-CHO yields ($P < 0.05$) and significant increases in AS yield per cell ($P < 0.05$; Fig. 2G and H) between growth and stationary phases, with the relative abundance of Glc significantly increasing ($P < 0.05$) in the HA fraction of both *Fragilariopsis* species (Fig. 4D; Table 1).

Comparison of monosaccharide composition EPS fraction and field data. Principal component analysis of the monosaccharide composition of the carbohydrate fractions and of natural sea-ice samples from the

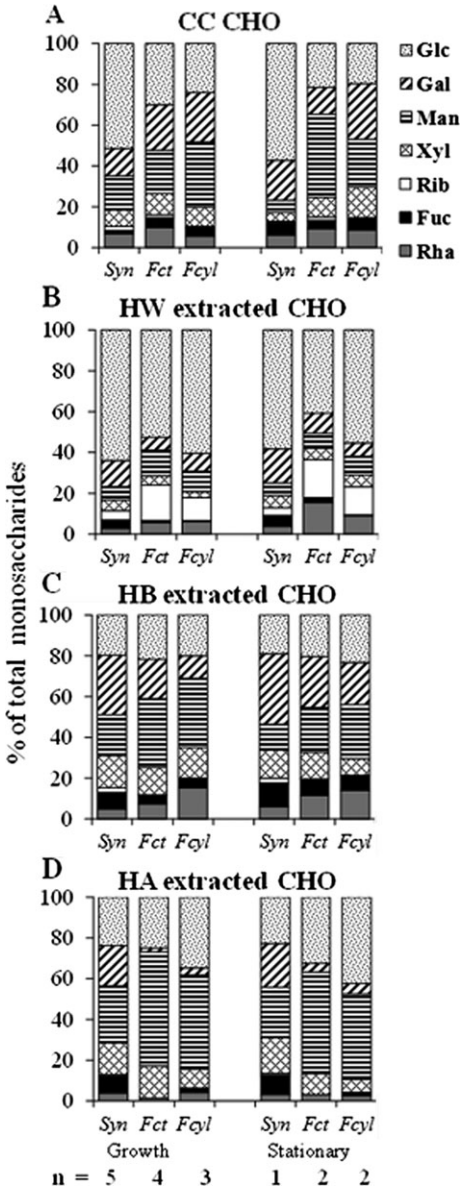

FIG. 4. Relative abundance of neutral sugar monosaccharides in dialyzed colloidal (CC), hot water (HW), hot bicarbonate (HB), and hot alkali (HA) carbohydrates (CHO) extracted from *Synedropsis* (*Syn*), *Fragilariopsis curta* (*Fct*), and *F. cylindrus* (*Fcyl*) during periods of active growth and stationary phases.

Weddell Sea, Antarctica (published in Underwood et al. 2010), identified a number of groupings (Fig. 5). Principal component 1 represented a gradient of decreasing relative abundance of Glc and increasing Gal, Fuc, and Xyl. HW and HB samples of all three diatom species were clustered at opposite ends of this gradient. CPs (CC) from *F. curta* and *F. cylindrus* were grouped with the HB samples and with sea-ice brines. Whole melted ice cores, algal-rich surface features (surface pools, slush, and gaps, see Underwood et al. 2010) were grouped at the glucose-rich end of this gradient, along with HW fractions from all three diatom species, and *Synedropsis* sp. CC. Principal component 2 represented a gradient of decreasing Man and Xyl and increasing Rib, Rha, and Gal, and separated the diatom HA from the CC and HW fractions (Fig. 5). Cluster Analysis (percent similarity) revealed two major groups (A and B; Fig. S2 in Supporting Information). Four subgroups of Cluster A contained (A1) the HA fractions from diatom frustules, but no field analogues; (A2) and (A3) were small groupings containing alcohol-fractionated sea-ice brines; and (A4) the majority of the ice brine samples, CC from both *Fragilariopsis* species and all HB fractions. Polysaccharides from melted Antarctic ice cores, HW samples (all diatom species), and *Synedropsis* CC were in cluster B and were characterized by high relative abundance of glucose and ribose (Fig. S2).

Effect of cold stress on growth and carbohydrate production by F. cylindrus. The intrinsic growth rate of *F. cylindrus* growing at 0°C was significantly lower at higher salinity (0.29 $d^{-1} \pm 0.01$ and 0.15 $d^{-1} \pm 0.025$ for 34 and 52 salinity cultures, respectively; Fig. 6). When temperature reduced to −4°C (d 13–16), growth rates declined further (0.10 $d^{-1} \pm 0.014$ and 0.03 $d^{-1} \pm 0.01$ for 34 and 52 salinity cultures, respectively). Some further growth occurred at 34 salinity over the next 13 d. All 34 salinity flasks froze when temperature was reduced to −8°C (Table S1 in the Supporting Information). Flasks containing 34 salinity media (no diatoms) froze at −4°C (Table S1). *F. cylindrus* grew slowly in 52 salinity media at −4°C, and growth ceased at −8°C (Fig. 6). 52 salinity cultures froze 1 d after temperatures were reduced to −12°C (d 40, Table S1), but 52 salinity media blanks froze at −8°C.

Yields of dissolved CC (pg C · $cell^{-1}$) in the 34 salinity cultures were comparable to yields in experiment 1 (Figs. 7 and 2A), but were three times higher for cells grown at 52 salinity (significant salinity effect in experiment 2, $P < 0.01$). There was no significant difference in HW carbohydrate yield per cell in the two salinity regimes, although values were lower than experiment 1. Yields of HB carbohydrate were lower than in experiment 1, but significantly more HB was produced by *F. cylindrus* grown at a salinity of 52. HA yields were significantly higher (at $P \leq 0.001$) in the 52 salinity treatment (Fig. 7), and similar to those measured in active growth in experiment 1, whereas 34 salinity-grown cells had HA yields similar to stationary phase *F. cylindrus* in experiment 1 (Figs. 7 and 2H).

Influence of high molecular weight polysaccharides (xanthan gum) on F. cylindrus *growth under cold stress.* Intrinsic growth rate of *F. cylindrus* was similar in controls and xanthan treatments at a salinity of 34 (0.25 $d^{-1} \pm 0.03$ and 0.25 $d^{-1} \pm 0.01$ for cultures with 1 and 5 g · L^{-1} xanthan, respectively) and 52 salinity (0.13 $d^{-1} \pm 0.01$ and 0.133 $d^{-1} \pm 0.003$ for cultures with 1 and 5 g · L^{-1} xanthan, respectively) at 0°C

TABLE 1. Summary of key features of PSA carbohydrate [CHO] and amino-sugar [AS] yields cell^{-1}, total carbohydrates, size fractions, ratios of carbohydrates, and monosaccharide composition, changes between growth and stationary phases, and differences between species for three ice diatom taxa, *Synedropsis* sp., *Fragilariopsis curta* and *F. cylindrus* grown in batch culture at 0°C, salinity 34, at 71 μmol photons · m^{-2} · s^{-1} irradiance.

Growth phases	Parameters	Extracellular CHO colloidal and EPS	Intracellular CHO hot water extract	Extracellular cell-bound CHO hot bicarb extract	Frustule-associated CHO hot alkali extract
Synedropsis					
Growth phase					
	% to ∑CHO	67%	24%	3%	6%
	[CHO]^{cell} yield	>*F. curta* and *F. cylindrus*	>*F. curta* and *F. cylindrus*		
	CHO:AS	14:1	4:1	3:2	2:1
	Monosaccharide (major sugars)	Glc	Glc	Gal Xyl, Man, Glc	Glc, Man, Gal, Xyl
	% CHO > 8 kDa	20%	n.d.	n.d.	n.d.
Stationary phase					
	% to ∑CHO	62%	23%	5%	10%
	CHO yield	↓[CHO]^{cell}, ↓[AS]^{cell}	↓[CHO]^{cell}, ↓[AS]^{cell}	↓[AS]^{cell}	
	CHO:AS	13:1	4:1	5:3	7:4
	Monosaccharide (changes)	↑Glc, ↑Gal, ↓Man	↓Glc	↓Man, ↑Fuc	↓Man, ↑Gal
	% CHO > 8 kDa	61%	n.d.	n.d.	n.d.
F. curta					
Growth phase					
	% to ∑CHO	75%	16%	6%	3%
	CHO yield	[AS]^{cell} > *Synedropsis*, *F. cylindrus*			
	CHO:AS	1:1	11:1	9:1	13:2
	Monosaccharide (major sugars)	Man, Gal, Glc	Glc and Rib	Glc, Gal, Xyl Man	Man, Glc, Xyl, Man
	% CHO > 8 kDa	35%	n.d.	n.d.	n.d.
Stationary phase					
	% to ∑CHO	79%	10%	5%	6%
	CHO yield	↓[CHO]^{cell}, ↓[AS]^{cell}	↓[CHO]^{cell}	↓[CHO]^{cell}, ↑[AS]^{cell}	↓[CHO]^{cell}, ↑[AS]^{cell}
	CHO:AS	1:1	3:1	8:3	1:1
	Stationary phase	↓Glc, ↓Man, ↑Gal,	↓Glc	↓Man, ↑Rha, ↑Fuc	↑Glc, ↑Rha, ↑Gal
	% CHO > 8 kDa	39%	n.d.	n.d.	n.d.
F. cylindrus					
Growth phase					
	% to ∑CHO	53%	21%	14%	12%
	CHO yield			[CHO]^{cell} > *Synedropsis F. curta* [AS]^{cell} > *Synedropsis F. curta*	[CHO]^{cell} > *Synedropsis F. curta* [AS]^{cell} > *Synedropsis F. curta*
	CHO:AS	14:1	11:1	4:1	2:1
	Monosaccharide		Glc and Rib rich	Glc, Gal, Xyl rich	Man and Glc rich
	% CHO > 8 kDa	67%	n.d.	n.d.	n.d.
Stationary phase					
	% to ∑CHO	40%	22%	23	15
	CHO yield		↓[CHO]^{cell}, ↑[AS]^{cell}	↓[CHO]^{cell}, ↑[AS]^{cell}	
	CHO:AS	11:1	7:2	1:2	4:5
	Monosaccharide	↓Glc, ↑Man	↓Glc		↑Glc
	% CHO > 8 kDa	78%	n.d.	n.d.	n.d.

(from d 0 to 13, Fig. 8). Reduction in temperature in 34 salinity treatments to −4°C caused a significant reduction in growth rates ($P < 0.001$, controls 0.10 d^{-1} ± 0.014; 5 g · L^{-1} xanthan treatment 0.03 d^{-1} ± 0.016), with growth virtually ceasing in 1 g · L^{-1} xanthan cultures. Both control and 1 g · L^{-1} xanthan 34 salinity treatments froze at −8°C (though 1 g · L^{-1} xanthan delayed freezing by 4 d, Table S1). Cell densities declined in the 5 g · L^{-1} xanthan treatment as temperatures were reduced to −8°C and −12°C, and cultures froze after 10 d at −12°C (Table S1).

The reduction in temperature to −4°C reduced intrinsic growth rates in 52 salinity cultures in both control (0.033 d^{-1} ± 0.015) and treatments (0.074 d^{-1} ± 0.05 and 0.05 d^{-1} ± 0.01 for 1 and 5 g · L^{-1} xanthan treatments between d 13 and 16, respectively). Cell densities continued to increase at very slow rates at −8°C until approximately d 33 (Fig. 8). Control cultures at salinity of 52 froze after 1 d at −12°C, with 1 g · L^{-1} xanthan cultures remaining liquid at −12°C for a further 10 d. Cultures at 52 salinity with 5 g · L^{-1} xanthan treatments froze 2 d after temperatures were reduced to −20°C (Table S1).

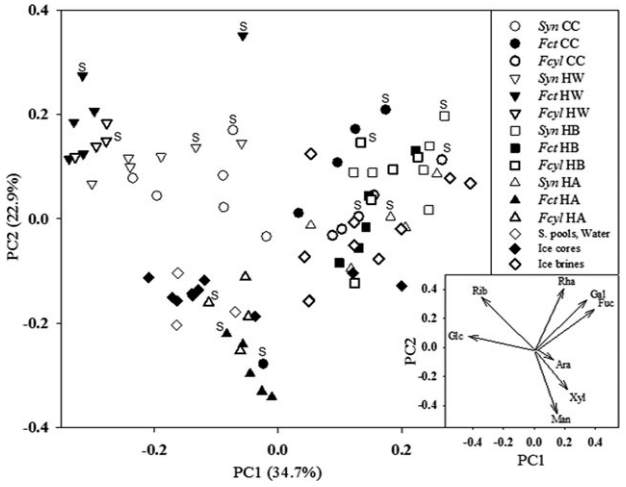

FIG. 5. Scatter plot of components 1 and 2 from principal components analysis of monosaccharide composition of different carbohydrate fractions from cultures of the polar diatoms *Synedropsis* (*Syn*), *Fragilariopsis curta* (*Fct*), and *F. cylindrus* (*Fcyl*) during active growth and during stationary phase (S), and from carbohydrate or EPS fractions measured in surface pools and features, in sea-ice cores and sea-ice brine samples from Antarctic sea ice during the 2004 ISPOL and 2006 WWOS cruises (data from Underwood et al. 2010). Vectors (inset) show the direction of increasing relative abundance of glucose (Glc), ribose (Rib), arabinose (Ara), rhamnose (Rha), galactose (Gal), fucose (Fuc), xylose (Xyl), and mannose (Man).

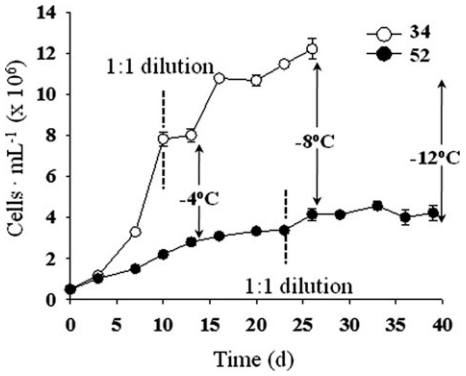

FIG. 6. Cell density of *Fragilariopsis cylindrus* under cold stress treatments in media of salinity 34 and 52 (mean ± standard error, $n = 3$ at each time point). Flasks were diluted (1:1) with fresh media after sampling on d 10 and 23 for salinity 34 and 52 treatments, respectively. Initial temperature was 0°C; temperature was lowered to −4°C on d 13, and further decreased to −8°C and −12°C on d 26 and 39, respectively. Cell enumeration ceased once cultures were frozen (mean ± standard error, $n = 3$ at each time point).

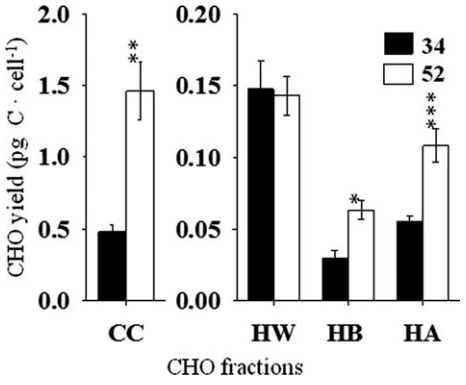

FIG. 7. Average yield (pg C · cell^{-1}) of phenol sulfuric acid quantified carbohydrates (PSA-CHO) in colloidal (CC), hot water (HW), hot bicarbonate (HB), and hot alkali (HA) fractions of *Fragilariopsis cylindrus* after 56 d, with temperatures reduced to −20°C at final sampling point (mean ± standard error, $n = 3$ at each time point for cell count, and $n = 6$ for carbohydrate analysis). *, **, and *** indicate significant differences between salinity treatments at $P < 0.05$, 0.01, and 0.001, respectively.

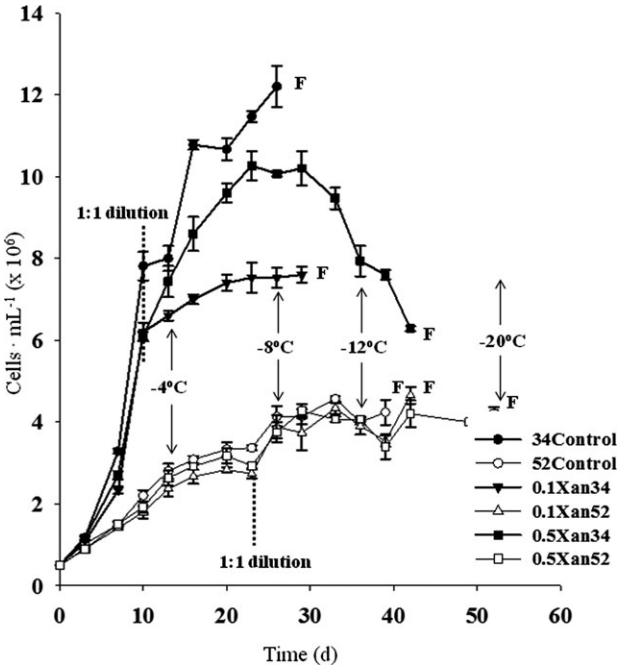

FIG. 8. Effect of additional polysaccharide in growth media (0 to control, 0.1% and 0.5% w/v xanthan) on *F. cylindrus* growth under cold stress (subzero levels) in media of salinity 34 and 52; Initial temperature 0°C; lowered to −4°C on d 13, further decreased to −8°C, −12°C, and finally to −20°C on d 26, 39, and 52, respectively. Cell counting for each culture was stopped after it was frozen (mean ± standard error, $n = 3$ at each time point).

DISCUSSION

The intrinsic growth rates for the three diatom taxa at 0°C were similar to those for *Nitzschia frigida* and *Thalassiosira antarctica* at −4°C (Aletsee and Jahnke 1992), although slightly lower than those for *F. cylindrus* at 0°C (Krell et al. 2007). Growth rates are temperature dependant and the decreases in rate we observed at lower temperatures agree with previously reported responses (Mock and Valentin 2004, Krell et al. 2007). Cultures had been acclimated previously to the irradiance used (71 μmol

photons · m^{-2} · s^{-1}; similar to low levels found in many sea-ice habitats; Søgaard et al. 2010, Petrou and Ralph 2011) and the fluorescence parameters provided no evidence of photoinhibition. All three taxa showed declines in F_v/F_m and increases in the effective cross-sectional area of PSII (σ_{PSII}) with time, indicative of decreasing nitrogen availability (Kolber et al. 1988, Bibby et al. 2008, Suggett et al. 2008), and corresponding slower growth, and changes in carbohydrate yields. Sea-ice diatoms can experience nutrient limitation within brine channels, associated with other physical and chemical changes, which induce a suite of physiological responses (Arrigo et al. 2010, Søgaard et al. 2010, Thomas et al. 2010). The growth experiments provide the evidence that there are differences in the characteristics of EPS secreted by ice diatoms when in active growth and when cells become nutrient limited.

EPS production by Synedropsis *sp.* F. curta *and* F. cylindrus. All three species produced colloidal extracellular heteropolysaccharides containing AS and with a complex monosaccharide composition. The constituent monosaccharides found were consistent with those of extracellular polysaccharides of other sea-ice (McConville et al. 1985, 1999) and benthic diatom species (e.g., Chiovitti et al. 2003, Underwood et al. 2004, Abdullahi et al. 2006). All three species had higher PSA-CHO yields in their growth phase compared with stationary phase, with significant differences in allocation between species, for example *Synedropsis* sp. produced higher concentrations of HW carbohydrates (both PSA-CHO and AS) whereas *F. cylindrus* produced higher levels of HB and HA carbohydrates. *F. curta* produced CC with a high proportion of AS. Amino sugars (constituents of the chitin spines of many centric diatoms) have rarely been detected in the soluble EPS from pennate diatom species (Chiovitti et al. 2003). Although the role that AS may play in EPS structural properties remains unclear, AS have been detected in soluble polysaccharides produced by bacteria (Mirelman et al. 1973, Orgambide et al. 1991) and fungi (Sandford et al. 1978). *Synedropsis* sp. produced high yields of extracellular dCHO compared to the *Fragilariopsis* species, but only 20% of this was polysaccharide >8 kDa in size. The CPs of *Synedropsis* sp. were mainly highly soluble EPS (% $CHO_{50–70}$) and non-EPS polysaccharides (% $CHO_{70–100}$). This contrasts to the high proportion of high molecular weight and insoluble EPS produced by the two *Fragilariopsis* species.

Hot water fractions were enriched with Glc in all three species, in accordance with other studies (McConville et al. 1986, Bhosle et al. 1995, Wustman et al. 1997, Staats et al. 1999, de Brouwer and Stal 2002, Chiovitti et al. 2003). Glc in HW extracts is mainly present as ß-1,3 linked glucan (chrysolaminarin), a major storage carbohydrate for many sea-ice diatom species (McConville 1985, McConville et al. 1986), and we assume that chrysolaminarin is the major polysaccharide in the HW extracts from *Synedropsis* sp. and *Fragilariopsis* spp. Ribose was also abundant in the HW extracts indicating some contamination with nucleic acid (Chiovitti et al. 2003). Other monosaccharides mainly Gal, Man, Xyl, and Rha were also detected in HW fraction. These monosaccharides could have an extracellular origin (Chiovitti et al. 2004, Abdullahi et al. 2006), as there are no reports of large quantities of any intracellular carbohydrate polymers other than chrysolaminarin in diatoms (Bellinger et al. 2005). Declines in yield and in Glc content of HW carbohydrate fractions are associated with lower rates of photosynthesis (de Brouwer and Stal 2002, Hanlon et al. 2006, Bellinger et al. 2009), and occurred when the cells entered stationary phase. Declines in glucan concentrations have also been found in natural Antarctic sea-ice assemblages during nutrient limitation (McConville et al. 1985).

There were no significant differences in the monosaccharide profiles of the CC and HB fractions for both *Fragilariopsis* species, though *Synedropsis* sp. HB did have a different composition compared to its CC fraction. The monosaccharide profiles of HB-extracted mucilages were heterogeneous, and dominated by Xyl, Man, and Gal, similar to the HB fractions of other diatom species (Chiovitti et al. 2005, Abdullahi et al. 2006). HB-EPS can form mucilage pads, stalks, and gels that stain strongly with alcian blue in culture (Abdullahi et al. 2006), and probably represent much of the particulate EPS, transparent exopolymer particles, and "mucilage sheets" observed in other culture and field studies (e.g., Aletsee and Jahnke 1992, McConville et al. 1999, Juhl et al. 2011, Krembs et al. 2011).

Both *Fragilariopsis* species produced high concentrations of AS in both HB and HA fractions, which increased during stationary phase (and in CC from *F. curta*). AS are also present in diatom cell wall-associated polysaccharides (McConville 1985, Durkin et al. 2009) and chitin is a main carbohydrate component within the silica cell walls of *Thalassiosira pseudonana* (Tesson et al. 2008). The AS-rich carbohydrate polymer produced by both *Fragilariopsis* species may be chitin, although this does require further characterization. The lack of ribose in the HB and HA extracts indicates that most soluble intracellular contaminants had been removed at this stage in the extraction series. Both *Fragilariopsis* species (but not *Synedropsis* sp.) produced a Man and Glc-rich HA fraction, indicating the possible presence of glucuronomannans. Substituted mannans with high concentrations of uronic acids are the most abundant polysaccharides extracted with hot alkali (Wustman et al. 1997, McConville et al. 1999, Chiovitti et al. 2005, Abdullahi et al. 2006), and are present in the thin organic casing attached to the siliceous wall (Volcani 1981). Although closely frustule associated, the HA fraction did exhibit changes in

composition during the shift into stationary phase, including substantial increases in AS. The HA fraction of *Phaeodactylum tricornutum* also changes (with more sulfate and uronic acid content) during both phosphorus limitation and salinity stress (Abdullahi et al. 2006).

The monosaccharide composition of EPS produced during growth phase differed to that in nutrient-limited stationary phase (McConville et al. 1999, Smith and Underwood 2000, Underwood et al. 2004, Abdullahi et al. 2006). Yields of CC declined in both *Fragilariopsis* taxa, with reduced Glc content in stationary phase, and more structural monosaccharides (xylose, mannose). Rheological properties of polysaccharides (gel formation) are dependent on physicochemical, structural (chain length, branching patterns) and environmental conditions (Suzuki and Tanaka 1990, Decho 1994, Chen and Hoffman 1995, Verdugo 2012). In *Synedropsis* sp., stationary phase CPs increased in Glc and Gal (low in gelling potential (Zhou et al. 1998, Giroldo et al. 2003), and decreased in Man (high gel potential), whereas for both *Fragilariopsis* species, structural monosaccharides such as xylose and mannose increased, changes that could contribute to increasing the gelling properties of *Fragilariopsis* polysaccharides in brine channels (Krembs et al. 2002).

We hypothesized that differences in the ecological niche of *Fragilariopsis* spp. and *Synedropsis* sp. would be reflected in differences in their EPS. This hypothesis was supported by the culture experiments, and by comparison of EPS monosaccharide profiles of cultures and carbohydrate fractions from natural sea ice (Fig. 5). It is possible that these are strain-specific differences, as we have worked with single strains of each diatom species and natural populations contain a range of genetic variability (Evans et al. 2005). However, both species within the genus *Fragilariopsis* showed greater similarity to each other than to *Synedropsis* sp., while Smith and Underwood (2000), using multiple fresh field isolates of five diatom species, found that EPS production and composition patterns were highly consistent within isolates of species.

Effect of cold stress and xanthan gum on growth kinetics and EPS production rates. Fragilariopsis cylindrus growth declined at both higher salinity and with decreasing temperatures. In broad agreement with other studies (cf. Aletsee and Jahnke 1992, Krell et al. 2007) growth did occur at −4°C but ceased at −8°C, in all treatments. Strategies employed by polar diatoms to remain physiologically active under lower temperatures and increasing salinity include altered protein expression, production of compatible solutes, and the production of antifreeze proteins (Mock 2002, Plettner 2002, Janech et al. 2006, Krell et al. 2007, Arrigo et al. 2010). *F. cylindrus* produced similar yields of the various carbohydrate fractions in the 34 salinity treatments in experiments 1 and 2, despite the temperature reductions in experiment 2. However, there were significantly higher yields in the CC, HB, and HB fractions at salinity 52. The diatoms *Phaeodactylum tricornutum* and *Cylindrotheca closterium* show similar plasticity in carbohydrate and EPS physiology, producing more carbohydrate (especially in HB and in EDTA-extracted fraction) under altered salinity conditions, and show altered motility, increased aggregation, and altered polymer chemistry (Abdullahi et al. 2006, Apoya-Horton et al. 2006).

Increased production rate of carbohydrates at low temperatures and higher salinity conditions, and altered EPS chemical composition when cell growth becomes limited (either by temperature, nutrients, or light) may be adaptations to resist freezing in brine channels (Krembs and Deming 2008). Increased carbohydrate production could increase habitable space in brine channels, as solutes are retained in sea ice by gelatinous EPS plugs, increasing the liquid brine fraction in sea ice (Krembs et al. 2002, 2011). The concentrations of dCHO reached in experiment 2 (243 and 247 μmol $C \cdot L^{-1}$) were equivalent to 4.9 and 5.1 mg Xan $\cdot L^{-1}$ (in 34 and 52 salinity cultures, respectively). These values match concentrations of dissolved and total carbohydrate reported for natural sea ice in both the Arctic and Antarctic (Dumont et al. 2009, Underwood et al. 2010, Juhl et al. 2011), although lower than total carbohydrate concentrations reported for bottom ice sections (up to 12 mg Xan $\cdot L^{-1}$ Krembs et al. 2011).

Addition of complex polysaccharides (xanthan gum) resulted in a further lowering of freezing temperature, in addition to the impact of the diatoms and their own secretions (including ice-binding proteins and other antifreeze components as well as polysaccharides, Janech et al. 2006, Arrigo et al. 2010). Addition of high molecular weight polysaccharide (xanthan) expanded the temperature "window" where media remained liquid from −8 to −12°C and from −12 to −20°C in 34 and 52 salinity cultures, respectively. Algal EPS, bacterial EPS, and xanthan gum all alter sea-ice formation, with natural EPS from the filamentous diatom *Melosira arctica* having the greatest influence on salt retention and increased brine-channel tortuosity (Krembs et al. 2011). The physics of ice formation in the presence of EPS (and its associated antifreeze proteins) is not well understood (Wettlaufer 2010), but an EPS matrix can reduce ice nucleation and crystal growth, creating a sphere on nonfreezing water bound up in a polysaccharide-electrolyte system surrounding cells (Krembs and Deming 2008), while potentially limiting algal growth due to restricted diffusion of nutrients (*F. cylindrus* had significantly lower growth rates, particularly once temperatures were reduced to −4°C, when in a matrix of xanthan gum). The more complex and insoluble EPS (in the CC, HB, and HA fractions) produced by *F. curta* and *F. cylindrus*, particularly when

cell growth is restricted, and enhanced at higher salinity would appear to fulfill the requirements of a protective gel.

Diatom EPS and sea-ice EPS. Polysaccharides can undergo reversible phase transitions from soluble forms into hydrated and then to condensed gels, in response to changes in the ionic, pH, and temperature conditions of the environment (Suzuki and Tanaka 1990, Decho 1994), and changes induced by the environment of the brine channel may lead to the formation of structures (e.g., physical gels) that provide protection for diatoms (Krembs and Deming 2008, Thomas et al. 2010, Verdugo 2012). Secretion of highly complex EPS in a dissolved form by diatoms (as seen in our experiments) may be a first response in their adaptation to the conditions of elevated salinity and freezing temperatures in sea-ice brines. Such extensive extracellular production would contribute to the observed strands and plugs of particulate gels seen in natural sea ice (Juhl et al. 2011, Krembs et al. 2011).

Similarity in monosaccharide composition of the *Fragilariopsis* HB and CC fractions (but not of the *Synedropsis* sp. CC) with that of brine samples from Antarctic sea ice (Underwood et al. 2010), suggests a relationship between these culture-derived diatom EPS and natural sea-ice material. HW fractions from all three diatoms were clustered with glucose-rich melted ice core samples and surface ice features (Fig. 5), both of which were associated with higher Chl *a* and/or lowermost ice layers in natural sea ice (Underwood et al. 2010). The carbohydrate content of melted ice cores was enriched in the more soluble EPS components, with high glucose content, particularly when algal biomass was high. Melted ice core samples may contain intracellular chrysolaminarin released by brine-channel diatoms, possibly due to nonfatal osmotic shocks during melting (Arrigo et al. 2010, Mikkelsen and Witkowski 2010). However, monosaccharide composition only provides basic information about the polysaccharides and more detailed structural analysis of these fractions is required to determine the structural similarities and differences in polysaccharides produced during different growth phases and present in natural sea ice.

CONCLUSION

This is the first study to characterize and compare the carbohydrates and EPS produced by three diatom species commonly associated with sea ice during different growth stages of growth. All three species produced chemically different heteropolysaccharides in both colloidal and cell-associated fractions; (highly complex EPS to non-EPS) with changes in the chemical composition of these polysaccharides produced by cells entering stationary phase in all cases. The sugar monosaccharide profiles of these different fractions had close similarity to EPS characterized in Antarctic sea ice. Both *Fragilariopsis* species produced highly complex EPS in comparison to *Synedropsis* sp., properties that would enhance survival of these taxa within sea-ice brine channels. Increased production of extracellular carbohydrates by diatom species appears to be a valid strategy to acclimate to cold stress under saline conditions. This hypothesis is further confirmed by the action of high molecular weight polysaccharides (xanthan) in resisting freezing and contributing to cell survival compared to cultures grown without xanthan. The actual mechanisms by which EPS enhance cell survival, and how these particular physiological responses are integrated with other known survival strategies of polar diatoms remain to be resolved, but our results support the hypothesis that diatom EPS plays an important protective role in the ecology of autotrophic biofilms growing on and within polar sea ice.

This work was supported by the U.K. Natural Environment Research Council (NE/E016251/1). We thank Dr. John Hallsworth, University of Belfast, Northern Ireland, Dr. Gerhard S. Dieckmann, Alfred-Wegener-Institute, Bremerhaven, Germany, and Dr. Thomas Mock, University of East Anglia, Norwich, U.K., for providing diatom strains. We thank Mr. John Green for all technical support for GC-MS analysis and Dr. Ben Green for PRIMER analysis, and the helpful comments of three anonymous reviewers.

Abdullahi, A. S., Underwood, G. J. C. & Gretz, M. R. 2006. Extracellular matrix assembly in diatoms (Bacillariophyceae). V. Environmental effects on polysaccharide synthesis in the model diatom, *Phaeodactylum tricornutum*. *J. Phycol.* 42: 363–78.

Aletsee, L. & Jahnke, J. 1992. Growth and productivity of the psychrophilic marine diatoms *Thalassiosira antarctica* Comber and *Nitzschia frigida* Grunow in batch cultures at temperatures below the freezing point of seawater. *Polar Biol.* 11:643–7.

Apoya-Horton, M. D., Yin, L., Underwood, G. J. C. & Gretz, M. R. 2006. Movement modalities and responses to environmental changes of the mudflat diatom *Cylindrotheca closterium* (Bacillariophyceae). *J. Phycol.* 42:379–90.

Arrigo, K. R., Mock, T. & Lizotte, M. P. 2010. Primary producers and sea ice. *In* Thomas, D. N. & Dieckmann, G. S. [Eds.] *Sea Ice*, 2nd ed. Wiley-Blackwell, Oxford, pp. 285–326.

Aslam, S. N., Underwood, G. J. C., Kaartokallio, H., Norman, L., Autio, R., Fischer, M., Kuosa, H., Dieckmann, G. S. & Thomas, D. N. 2012. Dissolved extracellular polymeric substance (dEPS) dynamics and bacterial growth during sea ice formation in an ice tank study. *Polar Biol.* 35:661–76.

Bellinger, B. J., Abdullahi, A. S., Gretz, M. R. & Underwood, G. J. C. 2005. Biofilm polymers: relationship between carbohydrate biopolymers from estuarine mudflats and unialgal cultures of benthic diatoms. *Aquat. Microb. Ecol.* 38:169–80.

Bellinger, B. J., Underwood, G. J. C., Ziegler, S. E. & Gretz, M. R. 2009. Significance of diatom-derived polymers in carbon flow dynamics within estuarine biofilms determined through isotopic enrichment. *Aquat. Microb. Ecol.* 55:169–87.

Berges, J. A., Franklin, D. J. & Harrison, P. J. 2001. Evolution of an artificial seawater medium: improvements in enriched seawater, artificial water over the last two decades. *J. Phycol.* 37:1138–45.

Bhosle, N. B., Sawant, S. S., Garg, A. & Wagh, A. B. 1995. Isolation and partial chemical-analysis of exopolysaccharides from the marine fouling diatom *Navicula subinflata*. *Bot. Marina* 38:103–10.

Bibby, T. S., Gorbunov, M. Y., Wyman, K. W. & Falkowski, P. G. 2008. Photosynthetic community responses to upwelling in

mesoscale eddies in the subtropical North Atlantic and Pacific Oceans. *Deep-Sea Res. Part II-Top. Stud. Oceanogr.* 55:1310–20.

de Brouwer, J. F. C. & Stal, L. J. 2002. Daily fluctuations of exopolymers in cultures of the benthic diatoms *Cylindrotheca closterium* and *Nitzschia* sp. (Bacillariophyceae). *J. Phycol.* 38:464–72.

Chen, G. & Hoffman, A. S. 1995. Graft copolymers that exhibit temperature-induced phase transitions over a wide range of pH. *Nature* 373:49–52.

Chiovitti, A., Harper, R. E., Willis, A., Bacic, A., Mulvaney, P. & Wetherbee, R. 2005. Variations in the substituted 3-linked mannans closely associated with the silicified walls of diatoms. *J. Phycol.* 41:1154–61.

Chiovitti, A., Higgins, M. J., Harper, R. E., Wetherbee, R. & Bacic, A. 2003. The complex polysaccharides of the raphid diatom *Pinnularia viridis* (Bacillariophyceae). *J. Phycol.* 39:543–54.

Chiovitti, A., Molino, P., Crawford, S. A., Teng, R. W., Spurck, T. & Wetherbee, R. 2004. The glucans extracted with warm water from diatoms are mainly derived from intracellular chrysolaminaran and not extracellular polysaccharides. *Eur. J. Phycol.* 39:117–28.

Decho, A. W. 1994 Molecular-scale events influencing the macroscale cohesiveness of exopolymers. *In* Krumbein, W. E., Paterson, D. M. & Stal, L. J. [Eds.] *Biostabilization of Sediments*, Bibliotheks und Informationssystem der Universität Oldenburg (BIS)—Verlag, Oldenburg, pp. 135–48.

Dubois, M., Gilles, K. A., Hamilton, J. K., Rebers, P. A. & Smith, F. 1956. Colorimetric method for determination of sugars and related substances. *Anal. Chem.* 28:350–6.

Dumont, I., Schoemann, V., Lannuzel, D., Chou, L., Tison, J. L. & Becquevort, S. 2009. Distribution and characterization of dissolved and particulate organic matter in Antarctic pack ice. *Polar Biol.* 32:733–50.

Durkin, C. A., Mock, T. & Armbrust, E. V. 2009. Chitin in diatoms and its association with the cell wall. *Eukaryot. Cell* 8:1038–50.

Evans, K. M., Kühn, S. F. & Hayes, P. K. 2005. High levels of genetic diversity and low levels of genetic differentiation in the North Sea *Pseudo-nitzschia pungens* (Bacillariphyceae) populations. *J. Phycol.* 41:506–14.

Ferrieres, L., Aslam, S. N., Cooper, R. M. & Clarke, D. J. 2007. The yjbEFGH locus in *Escherichia coli* K-12 is an operon encoding proteins involved in exopolysaccharide production. *Microbiol.* 153:1070–80.

Giroldo, D., Vieira, A. A. H. & Paulsen, B. S. 2003. Relative increase of deoxy sugars during microbial degradation of an extracellular polysaccharide released by a tropical freshwater *Thalassiosira* sp. (Bacillariophyceae). *J. Phycol.* 39:1109–15.

Gleitz, M., Bartsch, A., Dieckmann, G. & Eicken, H. 1998. Composition and succession of sea ice diatom assemblages in the Weddell Sea, Antarctica. *AGU Antarct. Res. Ser.*, 73, 107–20 (Antarctic Sea Ice Biological Processes, Interactions and Variability, edited by M. P. Lizotte and K. R. Arrigo).

Gleitz, M. & Thomas, D. N. 1992. Physiological-responses of a small Antarctic diatom (*Chaetoceros* sp.) to simulated environmental constraints associated with sea-ice formation. *Mar. Ecol. Prog. Ser.* 88:271–8.

Gleitz, M. & Thomas, D. N. 1993. Variation in phytoplankton standing stock, chemical-composition and physiology during sea ice formation in the south-eastern Weddell Sea, Antarctica. *J. Exp. Mar. Biol. Ecol.* 173:211–30.

Guillard, R. R. L. & Hargraves, P. E. 1993. *Stichochrysis immobilis* is a diatom, not a Chyrsophyte. *Phycologia* 32:234–6.

Günther, S. & Dieckmann, G. S. 2001. Vertical zonation and community transition of sea ice diatoms in fast ice and platelet layer, Weddell Sea, Antarctica. *Ann. Glaciol.* 33:287–96.

Hanlon, A. R. M., Bellinger, B., Haynes, K., Xiao, G., Hofmann, T. A., Gretz, M. R., Ball, A. S., Osborn, A. M. & Underwood, G. J. C. 2006. Dynamics of extracellular polymeric substance (EPS) production and loss in an estuarine, diatom dominated, microalgal biofilm over a tidal emersion-immersion period. *Limnol. Oceanogr.* 51:79–93.

Hasle, G. R., Medlin, L. K. & Syvertsen, E. E. 1994. *Synedropsis* gen-nov, a genus of araphid diatoms associated with sea ice. *Phycologia* 33:248–70.

Hoagland, K. D., Rosowski, J. R., Gretz, M. R. & Roemer, S. C. 1993. Diatom extracellular polymeric substances—function, fine-structure, chemistry, and physiology. *J. Phycol.* 29:537–66.

Janech, M. G., Krell, A., Mock, T., Kang, J.-S. & Raymond, J. A. 2006. Ice-binding proteins from sea ice diatoms (Bacillariophyceae). *J. Phycol.* 42:410–6.

Juhl, A. R., Krembs, C. & Meiners, K. M. 2011. Seasonal development and differential retention of ice algae and other organic fractions in first year Arctic sea ice. *Mar. Ecol. Prog. Ser.* 436:1–16.

Kang, S.-H. & Fryxell, G. A. 1992. *Fragilariopsis cylindrus* (Grunow) Krieger: the most abundant diatom in water column assemblages of Antarctic marginal ice edge zones. *Polar Biol.* 12:609–27.

Kolber, Z., Zehr, J. & Falkowski, P. 1988. Effects of growth irradiance and nitrogen limitation on photosynthetic energy conversion in photosystem-II. *Plant Physiol.* 88:923–9.

Krell, A., Beszteri, B., Dieckmann, G., Glockner, G., Valentin, K. & Mock, T. 2008. A new class of ice-binding proteins discovered in a salt-stress-induced cDNA library of the psychrophilic diatom *Fragilariopsis cylindrus* (Bacillariophyceae). *Eur. J. Phycol.* 43:423–33.

Krell, A., Funck, D., Plettner, I., John, U. & Dieckmann, G. 2007. Regulation of proline metabolism under salt stress in the psychrophilic diatom *Fragilariopsis cylindrus* (Bacillariophyceae). *J. Phycol.* 43:753–62.

Krembs, C. & Deming, J. W. 2008. The role of exopolymers in microbial adaptation to sea ice. *In* Margesin, R., Schinner, F., Marx, J. C. & Gerday, C. [Eds.] *Psychrophiles: From Biodiversity to Biotechnology*. Springer-Verlag, New York, pp. 247–64.

Krembs, C., Eicken, H. & Deming, J. W. 2011. Exopolymer alteration of physical properties of sea ice and implications for ice habitability and biogeochemistry in a warmer Arctic. *Proc. Natl Acad. Sci. USA* 108:3653–8.

Krembs, C., Eicken, H., Junge, K. & Deming, J. W. 2002. High concentrations of exopolymeric substances in Arctic winter sea ice: implications for the polar ocean carbon cycle and cryoprotection of diatoms. *Deep-Sea Res. I* 49:2163–81.

Kromkamp, J. C. & Forster, R. M. 2003. The use of variable fluorescence measurements in aquatic ecosystems: differences between multiple and single turnover measuring protocols and suggested terminology. *Eur. J. Phycol.* 38:103–12.

Levasseur, M., Thompson, P. A. & Harrison, P. J. 1993. Physiological acclimation of marine phytoplankton to different nitrogen sources. *J. Phycol.* 29:587–95.

Mancuso Nichols, C., Guezennec, J. & Bowman, J. 2005. Bacterial exopolysaccharides from extreme environments with special consideration of the Southern Ocean, sea ice, and deep sea hydrothermal vents: a review. *Mar. Biotechnol.* 7:253–71.

Marx, J. G., Carpenter, S. D. & Deming, J. W. 2009. Production of cryoprotectant extracellular polysaccharide substances (EPS) by the marine psychrophilic bacterium *Colwellia psychrerythraea* strain 34H under extreme conditions. *Can. J. Microbiol.* 55:63–72.

McConville, M. J. 1985. Chemical composition and biochemistry of sea ice microalgae. *In* Horner, R. I. [Ed.] *Sea Ice Biota*. CRC Press, Florida, pp. 106–29.

McConville, M. J., Bacic, A. & Clarke, A. E. 1986. Structural studies of chrysolaminaran from the ice diatom *Stauroneis amphioxys* (Gregory). *Carbohydr. Res.* 153:330–3.

McConville, M. J., Mitchell, C. & Wetherbee, R. 1985. Patterns of carbon assimilation in a microalgal community from annual sea ice, East Antarctica. *Polar Biol.* 4:135–41.

McConville, M. J., Wetherbee, R. & Bacic, A. 1999. Subcellular location and composition of the wall and secreted extracellular sulphated polysaccharides/proteoglycans of the diatom *Stauroneis amphioxys* Gregory. *Protoplasma* 206: 188–200.

Meiners, K., Gradinger, R., Fehling, J., Civitarese, G. & Spindler, M. 2003. Vertical distribution of exopolymer particles in sea ice of the Fram Strait (Arctic) during autumn. *Mar. Ecol. Prog. Ser.* 248:1–13.

van der Merwe, P., Lannuzel, D., Nichols, C. A. M., Meiners, K., Heil, P., Norman, L., Thomas, D. N. & Bowie, A. R. 2009. Biogeochemical observations during the winter spring transition in East Antarctic sea ice: evidence of iron and exopolysaccharide controls. *Mar. Chem.* 115:163–75.

Mikkelsen, D. M. & Witkowski, A. 2010. Melting sea ice for taxonomic analysis: a comparison of four melting procedures. *Polar Res.* 29:451–4.

Mirelman, D., Lotan, R., Bernsten, Y., Flowers, H. M. & Sharon, N. 1973. Purification and properties of an extracellular polysaccharide containing amino-sugars formed by *Bacillus cereus*. *J. Gen. Microbiol.* 77:5–10.

Mishra, A. & Jha, B. 2009. Isolation and characterization of extracellular polymeric substances from micro algae *Dunaliella salina* under salt stress. *Bioresour. Technol.* 100:3382 –6.

Mock, T. 2002. In situ primary production in young Antarctic sea ice. *Hydrobiologia* 470:127–32.

Mock, T. & Valentin, K. 2004. Photosynthesis and cold acclimation: molecular evidence from a polar diatom. *J. Phycol.* 40:732–41.

Nevot, M., Deroncele, V., Montes, M. J. & Mercade, E. 2008. Effect of incubation temperature on growth parameters of *Pseudoalteromonas antarctica* NF (3) and its production of extracellular polymeric substances. *J. App. Microbiol.* 105:255–63.

Orgambide, G., Montrozier, H., Servin, P., Roussel, J., Trigaletdemery, D. & Trigalet, A. 1991. High heterogeneity of the exopolysaccharides of *Pseudomonas solanacearum* strain gmi 1000 and the complete structure of the major polysaccharide. *J. Biol. Chem.* 266:8312–21.

Petrou, K. & Ralph, P. J. 2011. Photosynthesis and net primary productivity in three Antarctic diatoms: possible significance for their distribution in the Antarctic marine ecosystem. *Mar. Ecol. Prog. Ser.* 437:27–40.

Plettner, I. 2002. *Stressphysiologie bei antarktischen Diatomeen—Ökophysiologische Untersuchungen zur Bedeutung von Prolin bei der Anpassung an hohe Salinitäten und tiefe Temperaturen.* unpublished Ph.D. Thesis Universität Bremen, Germany.

Round, F. E., Crawford, R. M. & Mann, D. G. 1990. *The Diatoms: Biology and Morphology of the Genera.* Cambridge University Press, New York.

Sandford, P. A., Pittsley, J. E., Watson, P. R., Burton, K. A., Cadmus, M. C. & Jeanes, A. 1978. Rheological and other physical characteristics of polysaccharides from 2 black yeast like fungi. *J. Appl. Polym. Sci.* 22:701–10.

Smith, D. J. & Underwood, G. J. C. 2000. The production of extracellular carbohydrates by estuarine benthic diatoms: the effects of growth phase and light and dark treatment. *J. Phycol.* 36:321–33.

Søgaard, D. H., Kristensen, M., Rysgaard, S., Glud, R. N., Hansen, P. J. & Hilligsøe, K. M. 2010. Autotrophic and heterotrophic activity in Arctic first-year sea ice: seasonal study from Malene Bight, SW Greenland. *Mar. Ecol. Prog. Ser.* 419:31–45.

Staats, N., De Winder, B., Stal, L. J. & Mur, L. R. 1999. Isolation and characterization of extracellular polysaccharides from the epipelic diatoms *Cylindrotheca closterium* and *Navicula salinarum*. *Eur. J. Phycol.* 34:161–9.

Stickley, C. E., St John, K., Koc, N., Jordan, R. W., Passchier, S., Pearce, R. B. & Kearns, L. E. 2009. Evidence for middle Eocene Arctic sea ice from diatoms and ice rafted debris. *Nature* 460:376–88.

Suggett, D. J., Warner, M. E., Smith, D. J., Davey, P., Hennige, S. & Baker, N. R. 2008. Photosynthesis and production of hydrogen peroxide by *Symbiodinium* (Pyrrhophyta) phylotypes with different thermal tolerances. *J. Phycol.* 44:948–56.

Suzuki, A. & Tanaka, T. 1990. Phase transition in polymer gels induced by visible light. *Nature* 346:345–7.

Tesson, B., Masse, S., Laurent, G., Maquet, J., Livage, J., Martin-Jezequel, V. & Coradin, T. 2008. Contribution of multinuclear solid state NMR to the characterization of the *Thalassiosira pseudonana* diatom cell wall. *Anal. Bioanal. Chem.* 390:1889–98.

Thomas, D. N. & Dieckmann, G. S. 2002. Ocean science—Antarctic Sea ice—a habitat for extremophiles. *Science* 295:641–4.

Thomas, D. N., Kattner, G., Engbrodt, R., Gannelli, V., Kennedy, H., Haas, C. & Dieckmann, G. S. 2001. Dissolved organic matter in Antarctic sea ice. *Ann. Glaciol.* 33:297–303.

Thomas, D. N., Papadimitriou, S. & Michel, C. 2010. Biogeochemistry of sea ice. *In* Thomas, D. N. & Dieckmann, G. S. [Eds.] *Sea Ice*, 2nd ed. Wiley-Blackwell, Oxford, pp. 425–68.

Underwood, G. J. C., Boulcott, M., Raines, C. A. & Waldron, K. 2004. Environmental effects on exopolymer production by marine benthic diatoms: dynamics, changes in composition, and pathways of production. *J. Phycol.* 40:293–304.

Underwood, G. J. C., Fietz, S., Papadimitriou, S., Thomas, D. N. & Dieckmann, G. S. 2010. Distribution and composition of dissolved extracellular polymeric substances (EPS) in Antarctic sea ice. *Mar. Ecol. Prog. Ser.* 404:1–19.

Underwood, G. J. C. & Paterson, D. M. 2003. The importance of extracellular carbohydrate production by marine epipelic diatoms. *Adv. Bot. Res.* 40:183–240.

Verdugo, P. 2012. Marine microgels. *Annu. Rev. Mar. Sci.* 4: 375–400.

Volcani, B. E. 1981. Role of silicon in diatom metabolism and silicification. *In* Simpson, T. L. & Volcani, B. E. [Eds.] *Silicon and Siliceous Structures in Biological Systems.* Springer, New York, pp. 157–200.

Wettlaufer, J. S. 2010. Sea ice and astrobiology. *In* Thomas D, N. & Dieckmann, G. S. [Eds.] *Sea Ice an Introduction to its Physics, Chemistry, Biology and Geology.* Blackwell Science Ltd, Oxford, UK, pp. 579–94.

Wustman, B. A., Gretz, M. R. & Hoagland, K. D. 1997. Extracellular matrix assembly in diatoms (Bacillariophyceae).1. A model of adhesives based on chemical characterization and localization of polysaccharides from the marine diatom *Achnanthes longipes* and other diatoms. *Plant Physiol.* 113:1059–69.

Zhou, J., Mopper, K. & Passow, U. 1998. The role of surface active carbohydrates in the formation of transparent exopolymer particles by bubble adsorption of seawater. *Limnol. Oceanogr.* 43:1860–71.

Supporting Information

Additional Supporting Information may be found in the online version of this article at the publisher's web site:

Figure S1. Functional absorbance cross-section of PSII (σ_{PSII}) and the rate of reoxidation of the primary quinine acceptor QA) of *Synedropsis* sp., *F. curta,* and *F. cylindrus* cultures grown over 24 d (*Synedropsis* sp.) and 28 d (*Fragilariopsis* species) (mean ± standard error, $n = 3$ for each time point).

Figure S2. Scatter plot of components 1 and 2 from Principal Components Analysis of monosaccharide composition of different carbohydrate

fractions from cultures of the polar diatoms *Synedropsis* sp., *F. curta,* and *F. cylindrus* and from Antarctic sea-ice samples, coded by % similarity cluster analysis into groupings. Major groups (A and B) have a dissimilarity of 42% and internal similarity of 60% or greater. Cluster A contained four subgroups: A1 (36% dissimilar to the rest of cluster A, 70% similarity within group), clusters A2 and A3, and A4 (all > 80% similar within subgroups).

Table S1. Freezing temperatures for blanks and *F. cylindrus* cultures grown in different salinities (34S and 52S) without (control) and with xanthan treatments (1 and 5 g. L^{-1}).